

Simple Formulation of the Ultimate Lateral Resistance of Single Piles on Sand based on Active Pile Length

Mary Roxanne AGLIPAY¹, Kazuo KONAGAI², Takashi KIYOTA³ and Hiroyuki KYOKAWA⁴

¹Student Member of JSCE, Graduate Student, Institute of Industrial Science, University of Tokyo
(4-6-1 Komaba, Meguro-ku, Tokyo 153-8505, Japan)

E-mail:aglipay@iis.u-tokyo.ac.jp

²Fellow of JSCE, Professor, Graduate school of urban innovation, Yokohama National University
(79-1 Tokiwadai, Hodogaya-ku, Yokohama 240-8501, Japan)

E-mail:konagai@ynu.ac.jp

³Member of JSCE, Associate Professor, Institute Industrial Science, University of Tokyo
(4-6-1 Komaba, Meguro-ku, Tokyo 153-8505, Japan)

E-mail:kiyota@iis.u-tokyo.ac.jp

⁴Member of JSCE, Kajima Corporation

(1-3-1 Motoakasaka, Minato-ku, Tokyo 107-8388, Japan)

E-mail:kyokawa@kajima.com

Simulation of the in-situ behavior of pile foundation is necessary in the seismic design and assessment for target structural integrity and performance during earthquakes. Generally, the pile behavior is governed by its deformation. For commonly used flexible piles, this deformation is observed to be significantly greater at the upper region of the embedment length defined as the active pile length, L_a , and becomes negligible with increasing depth. To simply investigate the behavior response of a single pile embedded in a homogeneous sandy soil, a plane strain condition using the 2D finite element method in nonlinear analysis was done. The subloading t_{ij} model is used to model the elasto-plastic behavior of the soil and the pile is modeled as a 2D continuum-based beam element. Based on the rigorous solution, piles reach the ultimate state of its side soil under large lateral deformations. In this case, a soil wedge can be observed being pushed up along this active pile length. Therefore, a simplified method using the active pile length as a key parameter to describe the ultimate lateral resistance of piles embedded on sands is presented for more practical approach in the seismic design and assessment of piles.

Key Words: active pile length, ultimate pile lateral resistance, soil-pile interaction

1. INTRODUCTION

Piles are usually used as deep foundations for important structures, or structures supported by weak soils. These piles are most susceptible to external lateral loads like seismic motions. The lateral resistance of piles is generally governed by the soil-pile interaction since the movements of grouped piles and their side soils are mutually dependent on each other. When the piles are induced by a lateral load, they deform relative to the deformation of their surrounding side soil.

Many researches on soil pile interactions have been done especially in the advent of high computing powers where rigorous solutions can be done for any complex soil-pile configuration. However, it is still

warranted especially in the engineering practice that simple yet high caliber solutions can be available.

For flexible piles commonly used in engineering practice, the deformation of a vertical beam is observed to be significantly prominent at the upper portion of the embedment length and decreases with increasing depth. Within this region of deformation, the pile can be described as a cantilever beam, assuming fixity at negligible deformation. This region is called the active pile length¹⁾, L_a .

In the event of large seismic excitations, a soil wedge is pushed up as the pile deforms. The soil wedge along the active pile length is indicative of the ultimate lateral resistance. Therefore, a simplified expression for the ultimate lateral pile resistance can be described by active pile length for more practical

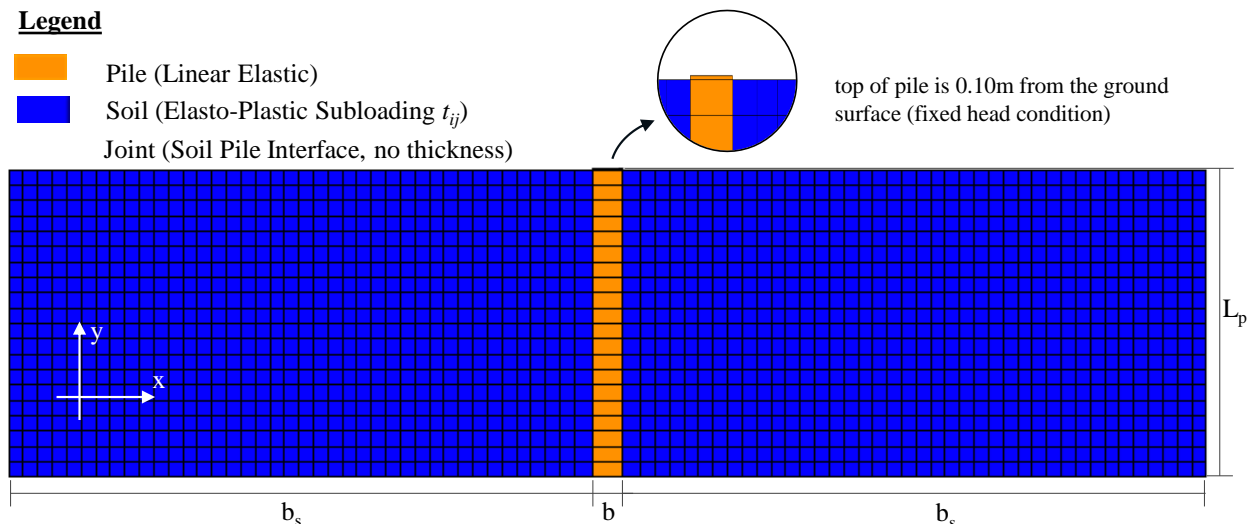


Fig 1 Soil-Pile System (not in scale)

approach in the seismic design and assessment of piles' performance.

2. NUMERICAL ANALYSIS

To investigate simply the idea of the nonlinear response of piles against the surrounding soil, the pile-soil system is modelled as 2D plane strain condition using the finite element method (see Fig.1). A single pile, of pile width, b , and length, L_p , is embedded in a homogeneous soil having a width, $b_s = 20\text{m}$, on opposite sides of the pile. In this case, the head of the pile is assumed fixed. The subloading t_{ij} model²⁾ is used to describe the elasto-plastic behavior of soils, while a continuum based beam element³⁾ is used for modelling the pile in elastic case. The pile head is slightly protruding from the ground level for the application of the lateral loading. The lateral load is applied monotonically until the pile head reaches 1.8m displacement. A joint element is introduced between the soil and the pile to simulate the vertical slipping of soil against the pile during nonlinearity. Separation between the soil and pile is not taken into account. The angle of internal friction of the joint element is 25° ⁴⁾. The bottom ends are considered as the hard strata, therefore, it is fixed in x and y directions. On the other hand, the sides are fixed only in x direction.

(1) Pile modeling

The end bearing pile is modeled as a vertical beam fixed in both directions at its bottom. Usually, in a finite element method, beams are modeled using line or quadrilateral elements. However, the use of continuum-based beam elements allows to capture the kinematics of the beam based on the Timoshenko

Beam Theory with smaller number of elements. Detailed discussion of the method is in ref 3.

Both the pile and its side soils are sliced into horizontal layers as illustrated in Fig. 1.

Parametric analysis was done to investigate the effect of pile width, b , Young's modulus of pile, E_p , and actual pile length, L_p , on the active pile length, L_a . The pile width, b , is varied from 0.3m to 2.0m. The elastic Young's modulus, E_p , of steel (200GPa) and concrete (30GPa) were considered. Generally, the length of the pile, L_p , used in this study is 30m.

(2) Soil modeling

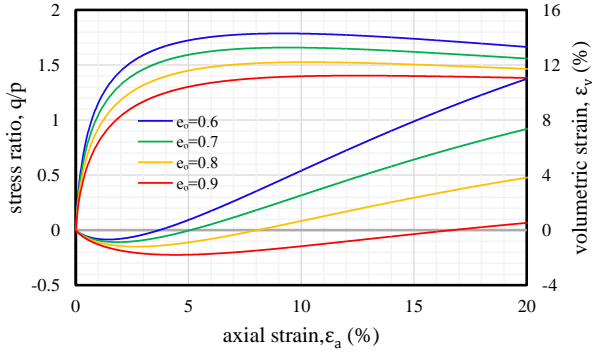
The elasto-plastic behavior of the side soil is modeled using the subloading t_{ij} model and incorporated in the finite element method. In this model, the intermediate principal stress and the influence of density on the strength and deformation of soil are accounted for. Detailed discussion about this model are found in ref 2..

The Toyoura sand (TS) is used as the homogeneous soil. The soil parameters were calibrated from the drained triaxial compression and extension results for loose and dense Toyoura sand⁵⁾. The soil parameters of Toyoura sand derived from the experiments are listed in Table 1.

The initial void ratios, e_o , are varied to 0.6, 0.7, 0.8 and 0.9. The corresponding stress paths and the volumetric strain-axial strain, $\varepsilon_v-\varepsilon_a$, relationship for varying void ratios are shown in Fig. 2. Generally, the dense sand exhibits a more dilatant behavior than loose sand. Piles on the loose ($e_o=0.9$) and dense ($e_o=0.6$) sand are investigated to see its effect on the active pile length.

Table 1 Soil Parameters of Toyoura Sand (TS)

| Material Parameters | |
|---|--------|
| compression index, λ | 0.070 |
| swelling index, κ | 0.0045 |
| stress ratio at critical state, R_{cs} | 3.2 |
| shape of yield surface, β | 2.0 |
| void ratio at normal consolidation at $P_a=98\text{kPa}$, e_{nc} | 1.10 |
| atmospheric pressure (kPa), P_a | 98 |
| controlling decay rate of the influence of density, a | 33 |
| poisson ratio, ν | 0.2 |

**Fig 2** Stress ratio- ε_a and ε_v - ε_a relationship of Toyoura sand with varying void ratios, e_o at $p'_o=98\text{kPa}$.

3. ACTIVE PILE LENGTH

The behavior of piles embedded in soil are generally governed by the deformation along its length. When the head of a flexible pile, which is commonly used in practice, is induced by a lateral loading, the deformation at the upper region along its length is remarkable. However it decreases with the increasing depth until it becomes negligible at some particular depth. Within this region of significant deformation, pile can be described as a cantilever beam, assuming fixity for the deeper region of negligible deformation.

In the engineering practice, the active length used for pile design is derived from Chang's formula⁶⁾ (Eq. 3a). This provides the measure of the stiffness of piles relative to the surrounding soil. Having a unit of m^{-1} , the inverse of this was thought of as characteristic length^{6),7)} of the pile, L_o as expressed in Eq. 3b

$$\beta = \sqrt[4]{\frac{k_h b}{4EI}} \quad (3a)$$

$$L_o = \frac{1}{\beta} \quad (3b)$$

where k_h coefficient of horizontal subgrade soil modulus

b pile width
 EI pile stiffness

The characteristic length in this case is a function of the coefficient of the horizontal subgrade soil modulus and the width of the pile. However, $k_h b$ is not an inherent characteristic of the soil but rather dependent on the pile geometric properties. Therefore, a more rational definition was proposed by Konagai¹⁾ to describe the pile deformation in terms of its stiffness with the surrounding soil stiffness given in Eq 3c.

$$L_o = \sqrt[4]{\frac{EI}{\mu}} \quad (3c)$$

where μ shear modulus of soil
 EI pile stiffness

This characteristic length is closely related to the active length by factor α as given by Eq. 3d. This is generally observed in some formulas proposed by proposed Randolph⁸⁾, Gazetas⁹⁾ and Velez¹⁰⁾.

$$L_a = \alpha L_o \quad (3d)$$

Practical classification of soil profiles are necessary to provide α for different soils¹⁾. However, Velez et al.¹⁰⁾ defined the active length, L_a , to be the length until at a point along the pile length where the pile's lateral displacement is 5% of the pile head displacement. Wang and Liao¹¹⁾ used 0.3% of the pile head displacement as the fixity point. In this paper, the point of fixity or zero bending is defined as 3% of the maximum pile head displacement.

(1) Effect of Pile Width, b

The active pile length is largely affected by the pile stiffness. Since the pile stiffness is a function of the pile geometric properties, the effect of pile width to the active length is investigated. In this case, a single pile with length, $L_p = 30\text{m}$, having an elastic Young's modulus of 30GPa, embedded in TS soil with initial void ratios of 0.6 and 0.9 were taken into account. While holding all parameters constant, the pile width, b , was set at 0.3m, 0.5m, 0.6m, 1.0m, 1.2m, 1.5m and 2.0m. This correspondingly varies the pile stiffness with respect to the same surrounding side soils.

Fig. 3 shows the variation of the pile width and its corresponding active pile length normalized with the actual pile length for piles embedded in the dense and loose condition. Generally, with increasing pile

width, the pile stiffness increases, and consequently, the active pile length increases. For piles with $L_a/L_p < 0.75$ and $b/L_p < 0.032$, the difference in the active pile length of piles embedded in loose and dense sands increases with increasing pile width. But when the b/L_p reached 0.032, where the ratio, L_a/L_p , becomes greater 0.75, the difference in the active lengths for piles embedded in loose and dense sand starts to decrease and converges to a point. In this scenario, as the pile becomes stiffer, the active length reaches the actual length. A saturation point starts to exist, where the active length becomes constant with increasing lateral pile head deformations as restrained by the fixity at the bottom of pile. In this study, flexible piles are of interests. Thus, piles having $L_a/L_p < 0.75$ are considered.

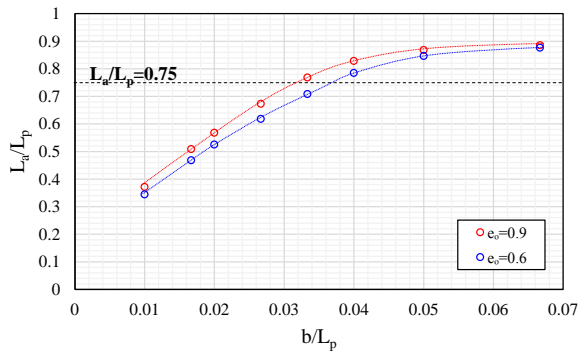


Fig 3 Normalized curve for the pile width, b , and active length, L_a , relationship.

(2) Effect of Young's Modulus of Pile, E_p

The piles having $E_p=200\text{GPa}$ with pile width, b , equal to 0.3m, 0.35m, 0.4m and 0.5m and embedded in loose Toyoura sand were considered. The obtained active pile lengths were superimposed to those of piles having $E_p=30\text{GPa}$ with pile width, b , equal to 0.3m, 0.5m, 0.6m and 0.8m. The elastic Young's modulus, E_p , directly affects the pile stiffness. Thus, increasing the Young's modulus, increases the active pile length.

The combined effect of the Young's modulus, E_p , and the pile width, b , using the pile stiffness parameter, EI , is plotted against the active pile length for all the cases considered in this particular parametric analysis. All the data points lie on a unique line defined by $y=2.891x + 3$, where y and x are the active pile length and $\sqrt[4]{EI}$ respectively. Note that the solid red points having $L_a/L_p > 0.75$ are not considered, as manifested by the rate of change in the slope of the pile stiffness and active pile length relationship due to the restraint at the bottom of piles. In this figure, it is established that $\sqrt[4]{EI}$ is indeed linearly proportional to the active pile length as expressed by eq 3c.

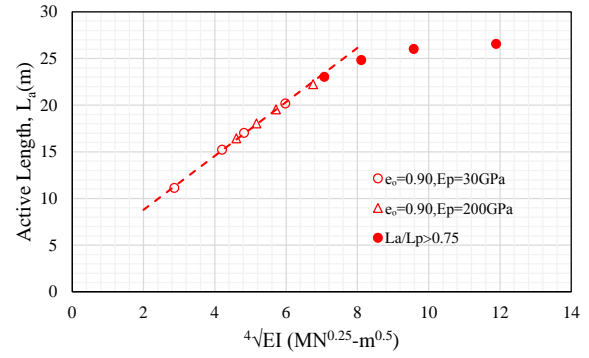


Fig 4 Effect of increase in pile stiffness, EI , on the active pile length, L_a .

(3) Effect of Pile Length, L_p

Now, the effect of variation of pile length on the active pile length is investigated. In this case, the single pile having stiffnesses of 312.5MN-m^2 and 2500MN-m^2 were taken into consideration. Each pile is embedded in the same loose sand condition, varying the pile lengths to 10m, 20m and 30m.

The result from this parametric study is shown in Fig. 5.

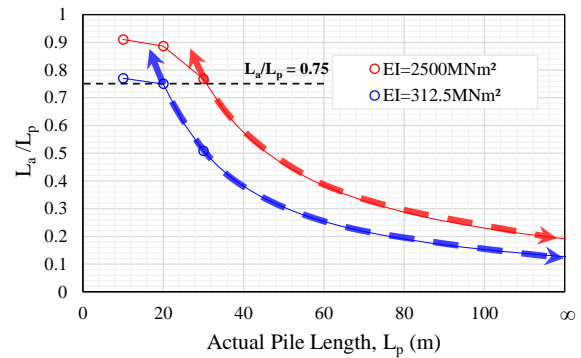


Fig 5 Effect of pile length, L_p , on the active pile length, L_a .

From this figure, it can be seen that for $L_a/L_p > 0.75$, described by the points on the solid line, the active pile length, L_a , continues to increase with increasing actual pile length, L_p . This can mean that the active length may actually need to be longer than the actual pile length but is restricted with the bottom boundary condition, thus behaving as stiff piles. However, as L_a/L_p becomes less than or equal to 0.75, the active pile length, L_a , starts to become constant despite increasing pile length, L_p as described by the red and blue broken lines. This shows an asymptotic behavior of L_a/L_p to 0 as L_p increases. It can mean that the supposed active pile length is reached given the actual pile length.

Figs. 6 and 7 show the lateral force at the pile head along the pile head displacements for different pile lengths.

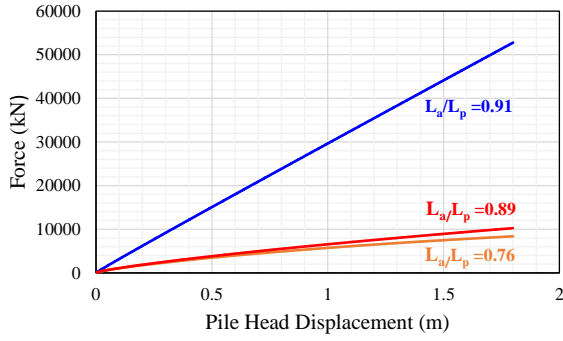


Fig 6 Lateral force at pile head along the pile head displacements for piles with varying lengths ($L_p = 10\text{m}, 20\text{m}, 30\text{m}$) having $EI = 2500\text{MNm}^2$

In Fig. 6, the lateral force at the pile head with $EI = 2500\text{MNm}^2$ have different responses for varying pile lengths. For piles with shorter length ($L_p = 10\text{m}$), there is a higher response at the pile head. This decreases with increasing the actual pile length, L_p , to 30m. With the same amount of force, the longer pile has more deformation capacity, thus the shorter pile exhibits a more stiffer behavior. Note that the short pile in this case, has ratio, L_a/L_p equal to 0.91 and as the L_a/L_p decreases to 0.75, the difference in the lateral force curves becomes smaller, i.e. in the case of piles having length equal to 20m and 30m. They have an L_a/L_p ratio of 0.89 and 0.77 respectively.

In Fig.7, the the lateral force at the pile head almost lie closely on a unique curve with for piles of varying length. In this case, their ratio L_a/L_p are approximately 0.75 and less.

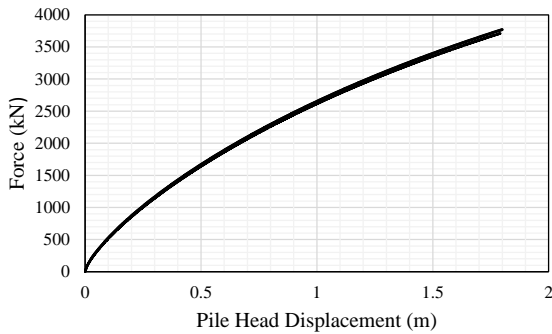


Fig 7 Lateral force at pile head along the pile head displacements for piles with varying lengths ($L_p = 10\text{m}, 20\text{m}, 30\text{m}$) having $EI = 312.5\text{MNm}^2$

This is in congruent in Fig. 3, where the change in trend was noticed. For $L_a/L_p < 0.75$, the difference in the active pile length of the piles embedded on the dense and loose sand increases with increasing pile width. However, at a point beyond $L_a/L_p = 0.75$, the points starts to converge. The fixity point starts to restricts the supposed formation of the active pile length. Thus, the pile behaves to be rigid and stiffer.

In this paper, flexible piles behaviour are of interests, therefore, the L_a/L_p to be taken into account shall be less than 0.75.

(4) Effect of Initial Void Ratio

The active pile lengths are derived for piles having different pile stiffnesses embedded on loose and dense sands for $L_a/L_p < 0.75$ as shown in Fig. 8.

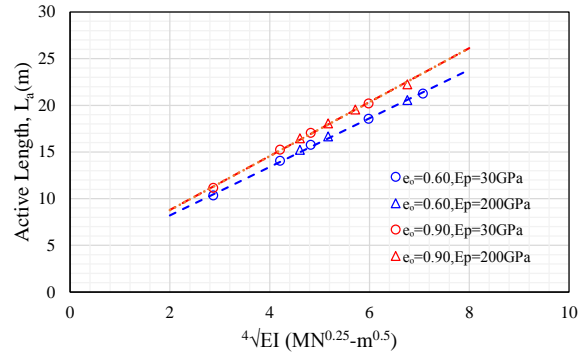


Fig 8 Effect of initial void ratio on the active pile length

All the data points for $e_0 = 0.90$ and $e_0 = 0.60$ lie on a unique line defined by $y = 2.891x + 3$ and $y = 2.601x + 3$ respectively, where y is the active pile length, L_a and the x is the fourth root of pile stiffness, $\sqrt[4]{EI}$. In this case, the active pile length of piles embedded in the loose sand are higher compared to the active pile length of piles embedded in the dense sands. The difference between the active pile length of piles embedded in dense and loose sands increases with increasing pile stiffness. This difference is associated with their behavior. Loose sands are easier mobilized with the progression of the active pile length compared to dense sand.

4. ULTIMATE SIDE SOIL RESISTANCE

Based from the numerical simulations, upon application of lateral load to the pile head at a rate of 0.002m/s, a triangular wedge is progressively formed at the passive region, at the same time an active wedge is moving with the pile. Along with the deformations of the pile, a local bulging around the pile surface appears upon reaching large deformations. In this event, soil in the passive region is being pushed upward with the soil surface not even with the pile head, indicating spillage over the pile in the real scenario. An example is seen in Fig. 9.

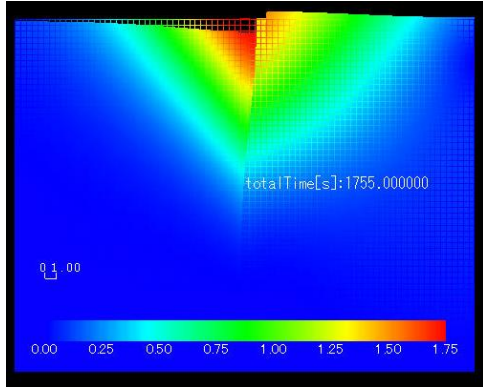


Fig 9 Displacement vector distribution of pile with $b=0.8m$, $E_p=30GPa$ embedded in loose TS induced with pile head displacement, $u_y=1.35m$

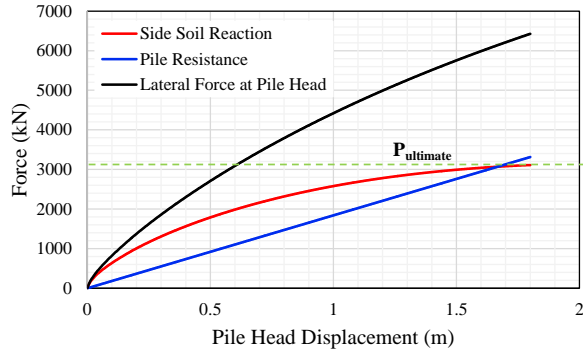


Fig 10 The lateral load-displacement relationship

Given the active length, the pile resistance can be derived assuming a cantilever beam of that length. The side soil reaction is derived from getting the difference between the curve of the lateral force at the pile head and the pile resistance based on active pile length. In Fig. 10, from the load-displacement curve of the side soil reaction, it can be observed that the side soil reaction becomes constant despite increasing pile head deformation, this constant value is the ultimate side soil reaction. The plateau region of the side soil resistance curve is found to be coincident at the starting point of the straight line after the non-linear phase of the load-displacement curve of the lateral force at the pile head. Thus, the active pile length is a key parameter to describe the ultimate lateral resistance of piles.

The force representation of the soil wedge can be defined by its unit weight, γ_d , and the Rankine passive earth coefficient, K_p . The following parameters are given by the following expressions.

$$\gamma_d = \frac{G_s \gamma_w}{1 + e_o} \quad (4a)$$

$$K_p = \tan^2\left(\frac{\pi}{2} + \frac{\phi}{2}\right) \quad (4b)$$

where G_s specific gravity of soil

γ_w unit weight of water ($9.81kN/m^3$)

ϕ angle of internal friction

The following soil parameters are used for the cases taken into account. The ϕ used is the peak angle of internal friction from the element test simulations.

Table 2 Soil Parameters of Toyoura Sand (TS) ($G_s = 2.65$)

| Initial void ratio, e_o | ϕ (deg) | γ_d (kN/m^3) |
|---------------------------|--------------|-------------------------|
| 0.60 | 43.51 | 16.25 |
| 0.70 | 40.53 | 15.29 |
| 0.80 | 37.47 | 14.44 |
| 0.90 | 34.67 | 13.68 |

Together with the active pile length, the soil parameters such as the unit weight of the soil (a function of the initial void ratio), Rankine passive coefficient, K_p are used to estimate the ultimate lateral resistance. Fig. 11 shows the correlation of the ultimate side soil reaction force and the parameters $K_p \gamma_d L_a$ for all the cases considered in this analysis having $L_a/L_p < 0.75$.

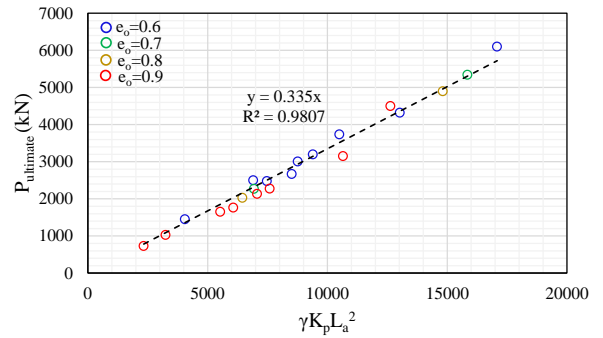


Fig. 11 Correlation between $P_{ultimate}$ and $K_p \gamma_d L_a^2$

In Fig. 11, there is a high correlation with the $P_{ultimate}$ and $\gamma_d K_p L_a^2$ having an $R^2=0.9807$. Therefore the $P_{ultimate}$ can be given by this equation:

$$P_{ult} = 0.335 K_p \gamma_d L_a^2 \quad (4c)$$

For sands

The side soil reaction curve is normalized with the eq. 4c and correspondingly, the pile head displacements with the active pile length as shown in Fig. 12. Two unique curves were observed. The one for $L_a/L_p > 0.70$ and for cases where $L_a/L_p < 0.70$. Here, it can be said that the $0.70 < L_a/L_p < 0.75$ is the transition phase for flexible to stiff piles. But generally, the simplified expression can describe the ultimate lateral pile resistance of flexible end bearing piles embedded in sands.

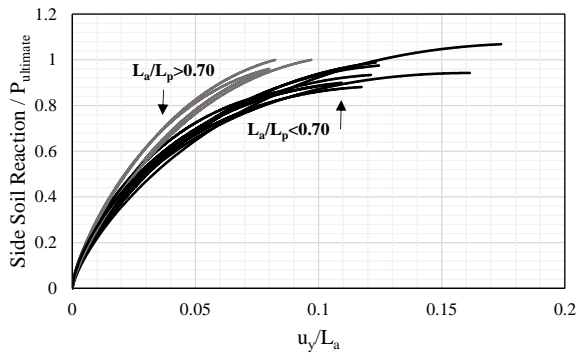


Fig. 12 Normalized Side Soil Reaction (TS)

5. CONCLUSIONS

The active pile length is generally governed by the stiffness of the pile relative to the surrounding soil stiffness. This is affected by the pile width, elastic Young's modulus, the pile length and the stress strain characteristics of the surrounding soil. To ensure use of flexible piles, $L_d/L_p < 0.75$ were taken into consideration to discount the limiting effect of the bottom boundary condition for shorter piles. The active pile length is linearly proportional to the fourth root of the pile stiffness. For piles having the same pile stiffness, it has higher active pile length when embedded in looser soil.

The use of active pile length to get the pile resistance and derive the side soil reaction from the load-deflection response curve at the pile head is indicative that the active pile length is a key parameter to define the ultimate lateral resistance. Together with other important soil parameters such as the soil unit weight and Rankine passive coefficient, the ultimate lateral resistance of the side soil can be estimated. This simplified expression can be useful for more practical approach in the seismic and assessment of piles. This idea can be extended to a more complicated scenario i.e. non-homogeneous soil, for group piles, etc.

ACKNOWLEDGMENT: The author would like to thank the Japanese government (Monbukagakusho : MEXT) for making this study possible through their financial support.

REFERENCES

- 1) Konagai, K., Yin, Y. and Murono, Y.: Single beam analogy for describing soil-pile group interaction, *Soil Dynamics and Earthquake Engineering*, Vol. 23, pp. 213-221, 2003.
- 2) Nakai, T., Kikumoto, M., Kyokawa H., Zhang, F. and Farias, M. : A simple and unified three-dimensional model to describe various characteristics of soils, *Soils and Foundations*, Vol. 51 No. 6, pp. 1149-1168, 2011.

- 3) Yoon K., Lee Y., and Lee, P.: A continuum mechanics based 3D beam finite element with warping displacements and its modelling capabilities, *Structural Engineering and Mechanics*, Vol. 43 No. 4, pp. 411-443, 2012.
- 4) Wakai A., Gose S. Ugai K.: 3-D elasto-plastic finite element analyses of pile foundations subjected to lateral loading, *Soils and Foundations*, Vol. 39 No. 1, 1999.
- 5) Kyokawa, H: Elastoplastic constitutive model for saturated and unsaturated soils considering deposited structure and anisotropy, *PhD Thesis*, 2011.
- 6) Chang YL.: Discussion on 'lateral piles loaded tests', *Feagin Trans, ASCE*, Vol. 1959, pp. 272-278, 1937.
- 7) Van Impe W., and Reese L.: Single piles and pile groups under lateral loading, Taylor & Francis, London, 2001.
- 8) Randolph MF: Response of flexible piles to lateral loading, *Geotechnique*, London, Vol. 315 No. 2, pp.247-259, 1981.
- 9) Gazetas G., and Dobry R.: Horizontal response of piles in layered soils, *J Geotech Engg, ASCE*, Vol. 110 No. 1, pp. 20-40, 1984.
- 10) Velez A., Gazetas G., Krishnan R.: Lateral dynamic response of constrained head piles, *J Geotech Engg, ASCE*, Vol. 109 No. 8, pp. 1063--81, 1983.
- 11) Wang MC, Liao WP.: . Active length of laterally loaded piles, *J Geotech Engg, ASCE*, Vol. 113 No. 9, pp. 1044-8, 1987.